

Optimized Embedding and Decoding of Extrinsic Signatures for Electrophotographic Halftone Images

Pei-Ju Chiang¹, George T.-C. Chiu¹, Edward J. Delp², and Jan P. Allebach²; School of Mechanical Engineering¹, School of Electrical and Computer Engineering², Purdue University, West Lafayette, Indiana/USA

Abstract

Printer identification based on a printed document can provide forensic information to protect copyright and verify authenticity. In this work, a stochastic dot interaction model that take in to consideration of scanner characteristics and print-scan channel noise is developed to predict the impact of embedding extrinsic signatures using laser intensity modulation. With this model, reflectance of the printout can be effectively estimated without extensive measurements. In addition, we proposed an optimization framework to select the modulation parameters that will maximize the embedding capacity and detection reliability. Preliminary analysis results such as achievable capacity and correct detection rate are discussed.

Introduction

To identify the printing device or authentication of the document, features such like banding or streaking generated by modulating EP process can be designed and utilized to help the extrinsic signatures. In previous work [1], we exploited the properties of pseudo-random noise (PN) sequences in developing associated embedding and detection algorithms. The unique cross-correlation properties of the PN sequence enabled decoding without the need of sequence synchronization [2], which improve the resistance of the proposed method to cropping attack. The embedding capacity can be increased by segmenting the image into rows with a different code embedded to each row.

Significant amount of printing and measurements are needed to identify the proper modulation parameters that are both time consuming and wasteful. A laser intensity modulation EP model [3] was developed to facilitate the development of optimal modulation parameters and reduce the required time and effort. Given a set of intensity modulation parameters, the model can effectively estimate the reflectance of the output image. With developed modulation model, Not only the image quality can be estimated but also the embedding and detection algorithm can be developed efficiently to increase the capacity and detection performance.

In this work, we will exercise the modulation model developed in [3] by including appropriate image process algorithms and a suitable image quality metric. An optimization problem is then formulated and solved to identify a set of modulation parameters that can maximize the embedding capacity while maintain image quality. The paper is organized as follows. Laser intensity modulation model will be discussed in the next section followed by the description of the image quality metric used in the study. Embedding algorithm and capacity analysis will be presented in the fourth section followed by the discussion of the detection algorithm. The optimization problem is described in the fifth section. Conclusions and future work are given in the last section.

Laser Intensity Modulation Model

In previous work [3], a laser intensity modulation model using stochastic dot interaction has been shown to be effective in predicting the reflectance of the halftone image for low embedding frequencies. The inclusion of the scanner modulation transfer function (MTF) can further improved the high frequency accuracy of the overall model. Figure 1 shows the proposed structure of the laser intensity modulation model for estimating the resulting image quality when embedding extrinsic signatures. In addition to the inclusion of the scanner MTF, a noise model is also developed to include the structured noise in the print-scan channel. In this section we will discuss the inclusion of the scanner MTF and the channel noise model in the overall system model.

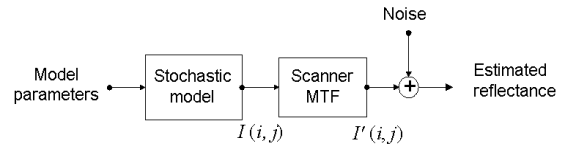


Figure 1. Block diagram of the laser intensity modulation model used in estimating the impact of signature embedding on image quality.

Scanner Modulation Transfer Function (MTF)

In this work, an Epson Perfection 3200 Photo with 600 dpi scanning resolution is used. To characterize the scanner MTF, a SINE M-13-60-1X pattern array is used as the test target. The detail instructions and techniques for characterize the MTF of a scanner can be found in [4]. Following [5], the scanner MTF is modeled as the weighted sum of two Gaussian functions, i.e.

$$B(\rho) = \alpha \exp\left(-\frac{\rho^2}{\sigma_1^2}\right) + (1 - \alpha) \exp\left(-\frac{\rho^2}{\sigma_2^2}\right), \quad (1)$$

where ρ is the 1-D frequency in cycles/in. Let the optimal weighting and standard deviations of two Gaussian functions with minimum mean square error (MSE) be α^* , σ_1^* and σ_2^* , respectively. Figure 2 shows the measured scanner MTF and the curve fitted scanner MTF model. A two-dimensional MTF of the scanner can be developed by substituting ρ^2 in (1) with $\rho^2 = u^2 + v^2$, where u is the spatial frequency in the process direction and v is the spatial frequency in the scan direction. the resulting 2-D MTF of the scanner can be presented as:

$$B(u, v) = \alpha^* \exp\left(-\frac{u^2 + v^2}{\sigma_1^{*2}}\right) + (1 - \alpha^*) \exp\left(-\frac{u^2 + v^2}{\sigma_2^{*2}}\right) \quad (2)$$

To facilitate the computation of the filtered image, the scanner MTF can be transferred to an equivalent point spread function (PSF). Convolution between the 2-D image $I(i, j)$ obtained from the previous stochastic model and the scanner PSF is used to obtain

the estimated scanned image $I'(i, j)$. The scanner PSF $b(x, y)$, where x is the scanner process direction and y is in the scanner scan direction, is obtained by using the scanner MTF in Eq. (2) as

$$b(x, y) = \alpha^* \pi \sigma_1^{*2} \exp(-\pi^2 \sigma_1^{*2} (x^2 + y^2)) + (1 - \alpha^*) \pi \sigma_2^{*2} \exp(-\pi^2 \sigma_2^{*2} (x^2 + y^2)) \quad (3)$$

After sampling and normalization with constant k such that the total area under the PSF is unity, the PSF of the scanner can be written as

$$b[m, n] = \kappa \alpha^* \pi \sigma_1^{*2} \exp(-\pi^2 \sigma_1^{*2} T^2 (m^2 + n^2)) + \kappa (1 - \alpha^*) \pi \sigma_2^{*2} \exp(-\pi^2 \sigma_2^{*2} (m^2 + n^2)) \quad (4)$$

Figure 3 shows the measured scanner point spread function. According to procedures in [2], the optimized model parameters are obtained by minimizing the error between measurements and estimated images $I'(i, j)$.

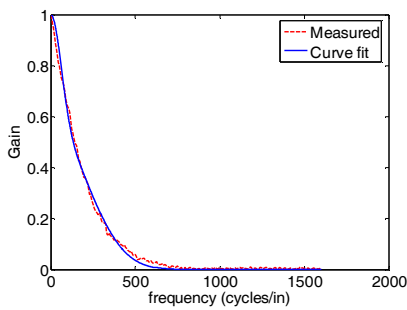


Figure 2. Measured and modeled scanner MTF

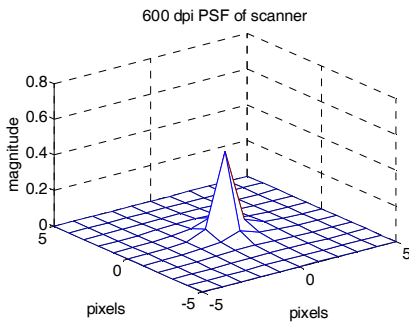


Figure 3. Scanner point spread function (PSF)

Noise Characterization

From communication channel point of view, the background noise will affect the signal to noise ratio (SNR) and subsequently the detection performance. To accurately estimate the image reflectance and optimize modulation parameters, including the noise of the printer-scanner channel in the model is essential.

To characterize the noise of the printer-scanner channel, digital halftoned image is printed by the printer with default setting without any modulation. The printed image is then scanned by a calibrated scanner. Since the halftone algorithm is coupled in the model, to measure the noise from the channel itself, the halftone frequency and its harmonics are filtered out from the scanned image. The measured noise is then injected into to the model to obtain the estimated reflectance. Figure 4(a) shows the FFT of the projection of the filtered scanned image and Fig. 4(b) is the noise of Fig. 4(a) in spatial domain.

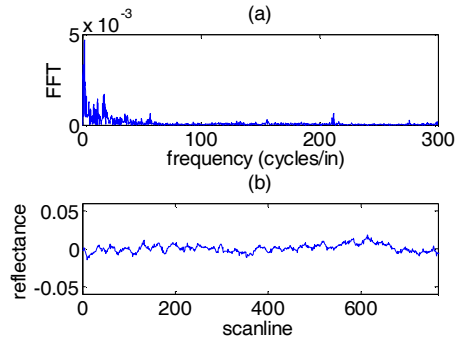


Figure 4. (a) DFT of measured communication noise, (b) Noise of (a) in spatial domain

With the inclusion of the scanner MTF and the noise model, the combined laser modulation model can precisely estimate the reflectance of the resulting halftoned images. Figure 5 shows the comparison between the measured and estimated images in one halftone screen.

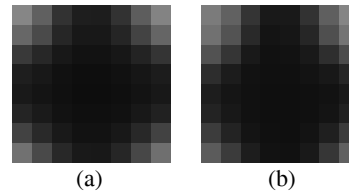


Figure 5. (a) Simulated image in one halftone screen (b) Printed image in one halftone screen

Image Quality

The embedding signal should not degrade image quality. To evaluate image quality, a well defined metric is needed. Figure 6 shows the process block diagram of quantifying the image quality. Since the current embedding method adjust the laser intensity scan-line by scan-line, the reflectance of a scanned image is projected on to the process direction to obtain a 1-D reflectance profile $S(j)$. Since modulating laser intensity results in dot gain modulation and change in luminance (contrast) of the image, the reflectance profile $S(j)$ will be filtered by the human contrast sensitivity function (CSF) to adjust for the impact of the human visual system. To emphasize the image quality affected by the embedding signal, a weighting filter W is applied to attenuate the halftone frequency and keeps other frequency components unaltered. Standard deviation q of the filtered signal is then used to quantify the image quality and can be calculated by

$$q = \text{std}[W[CSF[S(j)]]] \quad (5)$$

The lower value q means the less dispersive the image reflectance is in process direction.

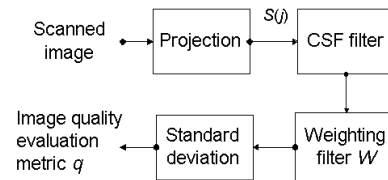


Figure 6. Process block diagram of quantifying image quality

Embedding Algorithm and Capacity

In our previous work, we assumed the position of the code is unknown and the encoded sequence with chip duration T_c and carrier frequency F_s is repeated throughout the entire image. The period of each Gold sequence is $T=2^n-1$ and $T_g = T_c \times T$ is the number of scan-lines used to present one complete cycle of embedding sequence. In this case, the embedding capacity is the set size of the Gold sequence generated by n -bits shift register that is around n -bits per image. To increase the capacity, the image can be divided into different rows with P scan-lines in the process direction. Each row can be embedded with a different sequence, see Fig. 7. To decode the embedding sequence, the number of scan-lines P in each row should be no less than T_g . To ensure the extracted image segment contains only one code with length no less than one period of embedding sequence, we allow a margin $S = P - T_g$ more scan-lines to embed the sequence in each row. The embedding length margin S depends on how precise the code position can be identified. Segments extracted from the row of image with length longer than T_g but shorter than P are then correlated with the potential code candidates. Majority vote is then used to elect the encoded code. Let the printer resolution be R_p lines per inch (lpi), the capacity (bits/in) can be calculated as

$$c(n, T_c, R_p, S) = \log_2[(2^n + 1)/(T_c(2^n - 1) + S)/R_p] \quad (6)$$

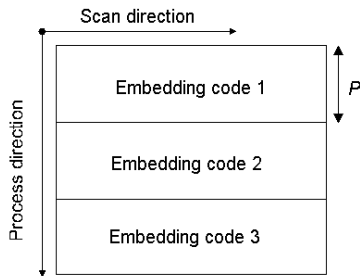


Figure 7. Images divided to different rows of images with length P and embedded with different code sequence

To maintain image quality, the embedding sequence is modulated with carrier frequencies F_s as mentioned in [1]. Table 1 lists the capacity for a 5 bit Gold sequence code and a margin $S=0$ with various chip duration T_c and corresponding carrier frequency F_s . To reduce the effect of printer modulation transfer function (MTF) and increase the reliability of detection, the chip duration cannot be too small. As can be seen from Table 1, there is a tradeoff between the capacity and detection rate, i.e. chip duration.

Table 1: Capacity of embedded sequence for $n=5$ with various chip duration T_c

T_c	F_s (cycles/in)	c (bits/in)
5	0, 120	19.53
6	0, 100	16.27
8	0, 75	12.20
10	0, 60, 120	9.76
12	0, 50, 100	8.14
15	0, 40, 80, 120	6.51

The embedding capacity also depends on the ability to precisely locate the code position in a scanned image. Figure 8 shows the decreasing capacity rate along with various length of margin S . If each embedded code can be precisely identified from

the image without any margin S , there is no decrease of the capacity. If $S=T_g$ more scan-lines are used to embed one sequence ($P=2T_g$), the capacity is decreased by half.

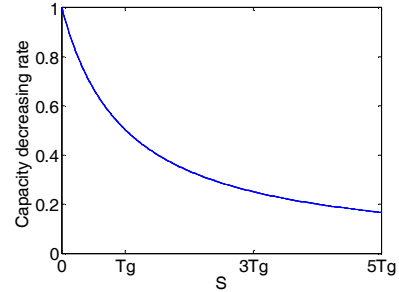


Figure 8. Capacity decreasing rate along with the embedding length margin S

Detection Algorithm

Noise rejection from the printed image will improve the detection efficiency and reliability. For a halftoned image, halftone noise is one of the most significant noise sources.

Rejecting Halftone Noise

During the printing process, halftone algorithm is applied to the image and coupled with the embedding signal. Since correlation is operated between the extracted signal and the sequence candidates, halftone noise coupled with extracted signal will degrade the maximum correlation value and reduce the detection reliability. To reduce the impact of halftone, a digital notch filter with narrow stop-band that passes most frequencies unaltered but attenuates the halftone frequency w_0 of the extracted signal to very low levels is applied. Figure 9(a) shows the embedding sequence with modulation parameters $n=5$, $T_c=10$, and $F_s=0$. Figure 9(b) shows the simulated filtered and unfiltered extracted signal with modulation amplitude $A = 0.2$ volt. The embedded sequence among the set of sequence candidates here is indexed as sequence 5. As shown in Fig. 9, the profile of the signal after filtering is much closer to the profile of embedding signal.

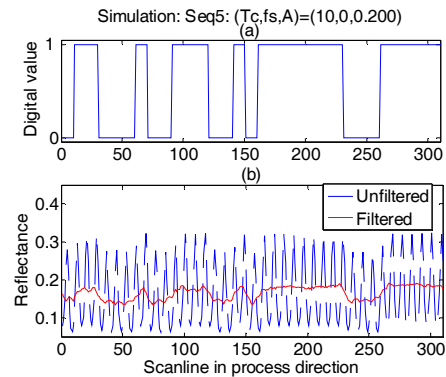


Figure 9. (a) Embedding sequence with $(T_c, F_s, A)=(10, 0)$ (b) Simulated extracted signal filtered and un-filtered with notch filter

Let \hat{X} be the decoded sequence, L be the set of code candidates X_i except the decoded code, and X the extracted data. The correlation ratio ε used to evaluate the detection performance is defined as

$$\varepsilon = \frac{\text{corr}(\hat{X}, X) - \frac{1}{|L|} \sum_{i \in L} \text{corr}(X_i, X)}{\text{std}\left(\frac{1}{|L|} \sum_{i \in L} \text{corr}(X_i, X)\right)}, \quad (7)$$

Figure 10 shows the correlation values of a simulated filtered and unfiltered extracted signal with all sequence candidates. As shown in Figure 10, the correlation value between filtered signal and sequence candidate 5 is much higher than the one without filtering. From Eq. (7), the correlation ratio for the unfiltered signal is 7.2824 and the one for the filtered signal is 12.6939 which is around 1.7 times higher. A higher correlation ratio will significantly improve the detection accuracy and reliability.

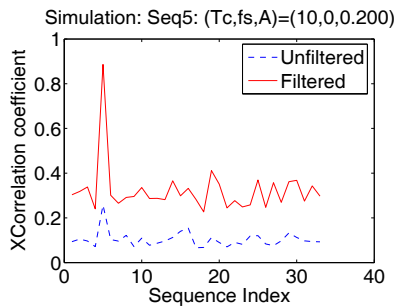


Figure 10. Correlation coefficient of simulated signal filtered and un-filtered with notch filter

Optimization of Modulation Parameters

With the proposed modulation model, reflectance of the printed halftone image can be effectively estimated without extensive measurements. In addition, with an off-line optimization framework, the modulation parameters can be optimized to enhance the capacity and detection accuracy and reliability. For a specific printer with resolution R_p , assuming that the n bit Gold sequence and the embedding length margin S are fixed, the embedding parameters that need to be determined are: the modulation amplitude A , the chip duration T_c , and the carrier frequency F_s . From previous discussion we see that the image quality q of an embedded image depends on both the modulation amplitude A and the carrier frequency F_s . From Eq. (6), the embedding capacity c depends on the chip duration T_c . In addition, the detection correlation ratio ε depends on the modulation amplitude A , chip duration T_c and carrier frequency F_s . To select the best set of modulation parameters such that the capacity is high, detection performance is reliable while maintaining the image quality, the following cost function is proposed

$$\Gamma = \frac{q}{\max(q)} - \frac{\varepsilon}{\max(\varepsilon)} - \frac{c}{\max(c)}. \quad (8)$$

Note that the above cost function is by no mean the best. It is used to illustrate the utility of such a model based approach to identify the optimal embedding parameter. The choice of a more appropriate cost function is the subject for future study. Based on the modulation model, the cost function of various modulation parameters are calculated and the optimal modulation parameters (A, T_c, F_s) are the set of parameters with minimum cost value as follows:

$$(A, T_c, F_s) = \min_{(A, T_c, F_s)} \Gamma, \quad (9)$$

There are several approaches to solve the optimization problem. Given the hardware limitations in the printer, the admissible chip durations and carrier frequencies are finite. To illustrate the utility of the procedure, we took the chip duration and carrier frequency values listed in Table 1. The range of modulation amplitude A is between 0.05 to 0.2 in 0.05 increments. Using the modulation model, the best set of modulation parameters that minimized the cost function (8) are $(A, T_c, F_s) = (0.2, 12, 50)$. With this set of optimal parameters, the achieved correlation ratio is 30.13 and the correlation coefficients of all sequence candidates are shown in Fig. 11. From Table 1, the achieved capacity is 8.14 bits per inch. However, the image quality q achieved is 0.009 which is higher than the q value without any information embedded. To sustain the image quality, in the future the elected modulation parameters for optimization should be constrained to those set with the value q equal or less than the one without any signatures, i.e. treating the image quality as an inequality constraint in the optimization problem. The optimal modulation parameters will be verified with the experimental results.

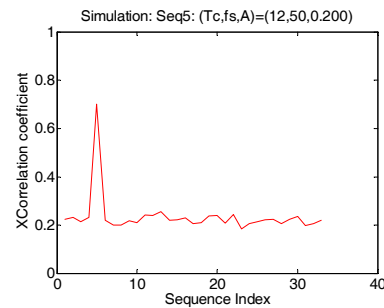


Figure 11. Correlation coefficient of simulated signal with optimized modulation parameters $(A, T_c, F_s) = (0.2, 12, 50)$

Conclusions and Future Work

In this work, the modulation model coupled with scanner MTF and print-scan channel noise is applied to estimate the image quality and detection correlation values for extrinsic signature embedding using laser intensity modulation. By segmenting the image into different rows with different embedded code sequences, the capacity is increased. In addition, by removing the impact of halftone noise in scanned data, the detection accuracy and reliability is significantly improved. By using the modulation model, an optimization problem can be formulated to identify the 'optimal' embedding parameters that will maximize the embedding capacity and detection accuracy and reliability while minimize the impact to image quality can be obtained. With the optimized modulation parameters, the achievable capacity is around 8 bits per inch. In the future, experiments will be conducted to verify the optimization results.

Acknowledgement

The authors would like to acknowledge the support of the National Science Foundation under the grant CCR-0524540.

References

- [1] P.-J. Chiang, A. K. Mikkilineni, S. Suh, G. T. C. Chiu, E. J. Delp, and J. P. Allebach, "Extrinsic Signatures Embedding and Detection in Electrophotographic Halftone Images through Laser Intensity

- Modulation,” Proceedings of NIP22: International Conference on Digital Printing Technologies, pp. 432-435, Denver, CO, September 17-22, 2006
- [2] M. B. Pursley, Introduction to Digital Communications, 2005 Pearson Education, Inc.
- [3] P. -J. Chiang, A. K. Mikkilineni, E. J. Delp, J. P. Allebach, G. T.-C. Chiu, “Development of an Electrophotographic Laser Intensity Modulation Model for Extrinsic Signature Embedding,” in the Proceedings of NIP 23: International Conference on Digital Printing Technologies, pp. 561-564, Anchorage, AK, September 16-21, 2007.
- [4] <http://www.mitre.org/tech/mf>
- [5] S.H. Kim and J.P. Allebach, “Optimal unsharp mask for image sharpening and noise removal,” Source: Journal of Electronic Imaging, v 14, n 2, April 2005, p 23005-1-13

Author Biography

Pei-Ju Chiang received the B.S. degree in Mechanical and Marine Engineering from National Taiwan Ocean University, in 1999, and her M.S. degree in Mechanical Engineering from National Central University, in 2001. She is currently a Ph.D. candidate in the School of Mechanical Engineering at Purdue University, West Lafayette. She is a student member of IS&T and ASME.